CHEMISTRY
AN ASIAN JOURNAL
ACES
FULL PAPER

DOI: 10.1002/asia.201201089

Facile Synthesis and Photophysical Properties of Sphere–Square Shape Amphiphiles Based on Porphyrin–[60]Fullerene Conjugates

Chien-Lung Wang,*[a, b] Wen-Bin Zhang,[a] Xinfei Yu,[a] Kan Yue,[a] Hao-Jun Sun,[a] Chih-Hao Hsu,[a] Chain-Shu Hsu,[b] Jojo Joseph,[c] David A. Modarelli,*[c] and Stephen Z. D. Cheng*[a]

Abstract: Molecules constructed from a combination of zero-dimensional ([60]fullerene (C_{60})) and two-dimensional (porphyrin (Por)) nanobuilding blocks represent an intriguing category of sphere–square "shape amphiphiles". These sphere–square shape amphiphiles possess interesting optoelectronic properties. To efficiently synthesize a large variety of C_{60}–Por shape amphiphiles, a facile route based on Steglich esterification was developed. The synthetic strategy enables the preparation of hydroxy-functionalized Por precursors (**9**–**12**) with high purity in a one-pot procedure. All of the C_{60}–Por shape amphiphiles (**1**–**5**) can be readily synthesized in good yields through subsequent Steglich esterification with a highly soluble carboxylic acid derivative of methanofullerene (**13**). Photophysical studies indicated weak electronic coupling between the C_{60} and Por moieties and suggest an edge-to-face alignment for the moieties. The fluorescence of electronically excited Por portions of each amphiphile was efficiently quenched, which was indicative of electron transfer from ^{1}Por to the C_{60} group(s). Increasing the number of C_{60} groups on the shape amphiphiles led to more pronounced quenching of the Por fluorescence, which indicated the potential for more effective generation of charge-separated species, $C_{60}^{-\bullet}$–$Por^{+\bullet}$, from the photoexcited C_{60}–Por shape amphiphiles.

Keywords: fullerenes · photophysics · porphyrinoids · shape amphiphiles

Introduction

Driven by noncovalent interactions, self-assembling processes are recognized as one of the most important ways to build up complex supramolecular entities.[1–7] Based on self-assembly principles, various complex functional supramolecular materials have been developed.[8–14] The synergy between geometric complementarity and noncovalent interactions is the determining factor in the formation of the final structure. Based on dimensionality and geometry, nanobuilding blocks can be generally divided into four categories: spheres (0D), cylinders (1D), discs (2D), and bulk complex structures (3D). Molecules consisting of geometrically distinct subunits are thus known as "shape amphiphiles".[15–27] Because the covalent linkage changes not only the geometry, but also the symmetry of the molecules, the molecular shape is also an important factor in tuning the final self-assembled structures in addition to noncovalent interactions.

Porphyrin (Por) and [60]fullerene (C_{60}) are representative 2D and 0D conjugated nanobuilding blocks (Scheme 1). Although the major noncovalent interactions are both π–π interactions, the shape and geometry define the favorable interaction orientations and the resulting supramolecular architectures. The 2D nanobuilding block, Por, prefers to form columnar phases through directional face-to-face π–π stacking,[28,29] whereas the 0D sphere, C_{60}, favors the formation of a plastic crystal phase with a face-centered cubic unit cell, in which the π–π interaction is anisotropic.[30] Covalently bound Por and C_{60} breaks the centrosymmetry of the original nanobuilding blocks and gives a series of intriguing Por–C_{60} shape amphiphilies.[31–38] In terms of functionality, covalently bound Por and C_{60} forms an electron donor–acceptor dyad. Unique photophysical properties, such as ultrafast photoinduced charge separation, long-lived charge-separation state, ambipolar charge transport, and photovoltaic activities, demonstrated the potential of C_{60}–Por shape amphiphiles in optoelectronic applications.[34,36,37,39–43]

[a] Prof. C.-L. Wang, W.-B. Zhang, X. Yu, K. Yue, H.-J. Sun, C.-H. Hsu, Prof. S. Z. D. Cheng
Department of Polymer Science
College of Polymer Science and Polymer Engineering
The University of Akron, Akron, Ohio 44325 (USA)
E-mail: scheng@uakron.edu

[b] Prof. C.-L. Wang, Prof. C.-S. Hsu
Department of Applied Chemistry, National Chiao Tung University
1001 Ta Hsueh Road, Hsinchu 30010 (Taiwan)
E-mail: kclwang@nctu.edu.tw

[c] J. Joseph, Prof. D. A. Modarelli
Department of Chemistry and The Center for Laser and Optical Spectroscopy, Knight Chemical Laboratory
The University of Akron, Akron, Ohio 44325-3601 (USA)
E-mail: dmodarelli@uakron.edu

Supporting information for this article is available on the WWW under http://dx.doi.org/10.1002/asia.201201089.

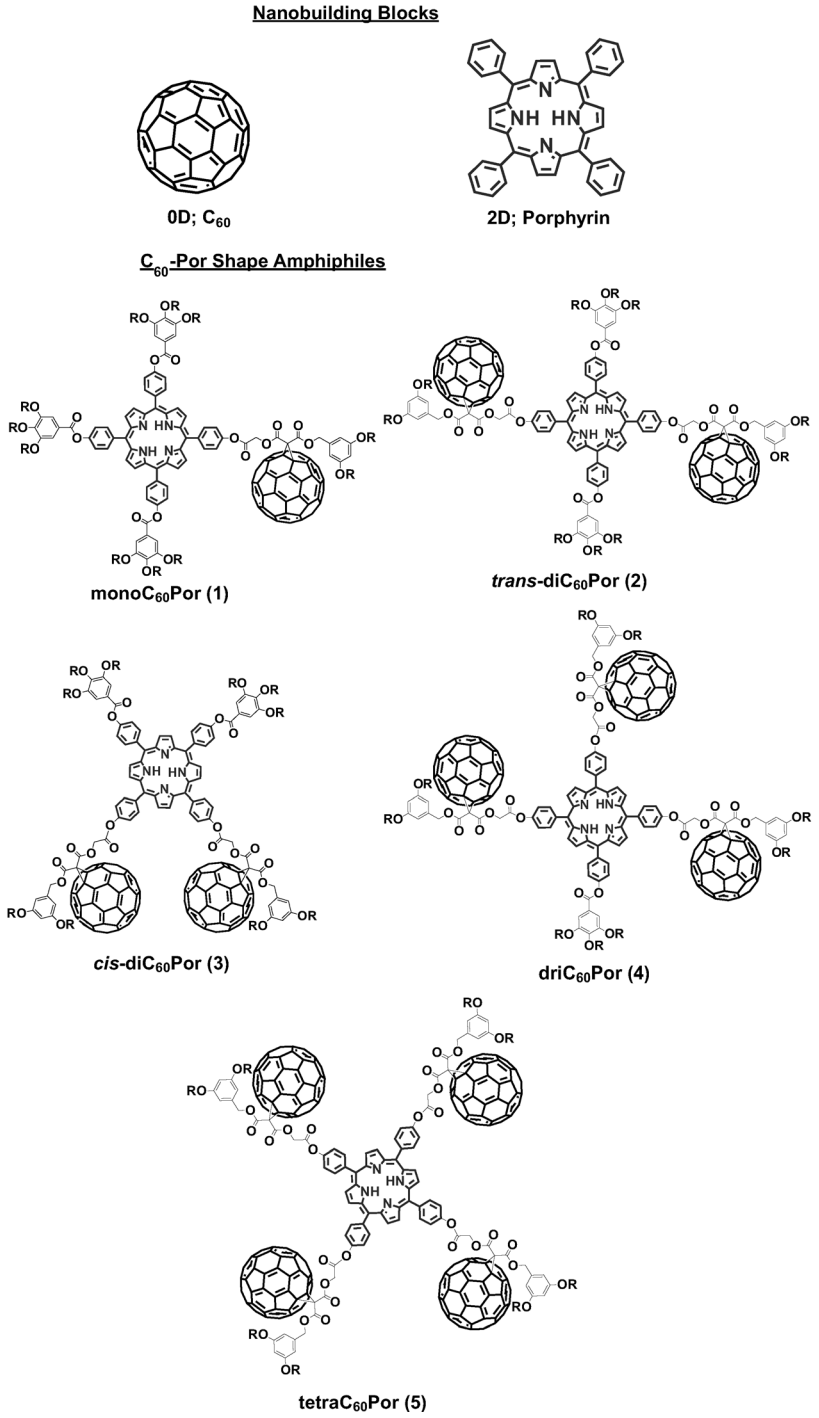

Scheme 1. Molecular structures of C_{60}, the Por nanobuilding blocks, and the C_{60}–Por shape amphiphiles.

Recently, we reported our efforts toward self-assembled, hierarchical "double cable" supramolecular structures in the bulk through the design and synthesis of Por–C_{60} shape amphiphiles.[44–46] These shape amphiphiles first form hierarchical "double cable" columns and further organize into 3D orthorhombic or hexagonal columnar lattices.[45,46] An alternating arrangement of Por and C_{60} in a triclinic lattice formed by *trans*-diC_{60}–Zn^{II}Por was also observed.[44] These studies demonstrated an abundance of supramolecular entities formed by C_{60}–Por shape amphiphiles and their potential use in optoelectronic applications. Because an efficient and precise synthesis is a prerequisite in the study of structure–property relationships, our attention focused on extending the previously reported two-step esterification strategy to the synthesis of a library of C_{60}–Por shape amphiphiles for a systematic study. The structures are thus constructed with a single Por core, as shown in Scheme 1. It is evident that, not only the chemical compositions (C_{60}/Por ratio per molecule), but also the molecular geometries, can be systematically varied. Intriguing optoelectronic and self-assembly behavior of these molecules is anticipated.

The synthesis of Por–C_{60} conjugates mainly involves two approaches: 1) condensation of a C_{60}-containing component to form the Por core;[47–49] and 2) attaching C_{60} to a preformed functionalized Por.[50] The preparation of Pors through the condensation of aldehyde and pyrrole is known to give a mixture of compounds that are usually difficult to separate.[51,52] The synthesis of Por–C_{60} by using the first method is thus costly. The post-functionalization method circumvents the difficulties associated with Por synthesis and has become prevalent. However, this approach is also limited by the low solubility of both Por and C_{60} and the functional group tolerance of the coupling reaction when considering the multitude of functional groups in the system. Recently, click chemistry has been applied to the synthesis of such a construct with a triazole linkage.[53–57] Our approach uses a two-step esterification process and introduces 3,4,5-trisdodecyloxy benzoate and 3,5-bis(dodecyloxy)benzyl groups with long alkyl groups to make both components highly soluble, thereby facilitating the synthesis and purification of the final molecule.

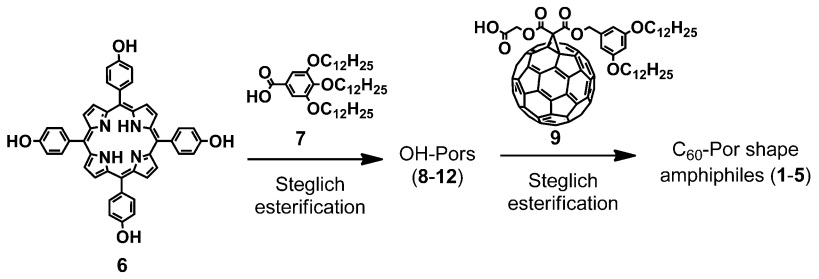

Scheme 2. The two-step synthetic route for preparing the C_{60}–Por amphiphiles.

Herein, sequential esterification strategies were used to effectively generate a library of C_{60}–Por shape amphiphiles. First, 5,10,15,20-tetra(*p*-hydroxyphenyl)porphyrin (**6**) was chosen as the core unit and Steglich esterification was used to sequentially connect the peripheral substituents, which were 3,4,5-trisdodecyloxybenzoic acid (**7**) and a carboxylic acid derivative of methanofullerene (**13**).[58] By taking advantage of the large polarity difference between the hydroxy group and the ester group, all of the specifically hydroxy-functionalized porphyrins (OH-Pors in Scheme 2) can be prepared effectively and separated easily in a one-pot reaction. The C_{60}–Por shape amphiphiles were then synthesized by treating the OH-Pors with **13** through a second Steglich esterification. This synthetic procedure has the following advantages: First, control of the number of functional groups per Por is achieved at an early stage of the synthesis. As shown in Scheme 3, monoOH-Por (**9**), 5,15-diOH-Por (**10**), 5,10-diOH-Por (**11**), and 5,10,15-triOH-Por (**12**) were separated and obtained during the first step of the synthesis. Second, the carboxylic acid derivative of methanofullerene, which is more time-consuming and costly to prepare, is only used in the last step of the synthesis. Third, the mild reaction conditions of Steglich esterification prevent potential decomposition in the reaction to the conjugated molecules.

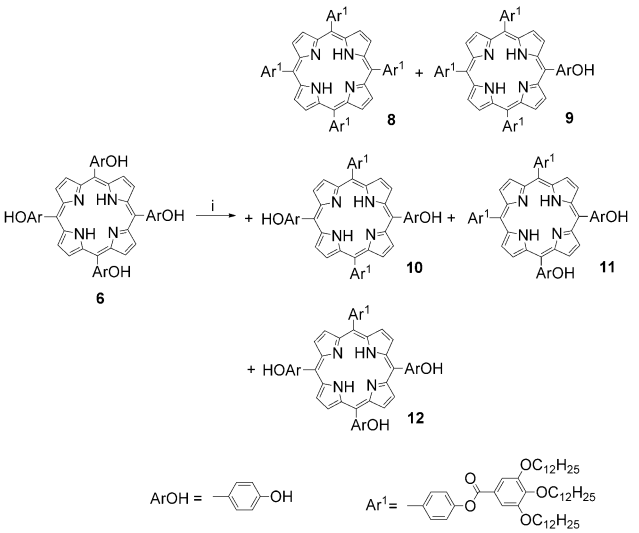

Scheme 3. Synthetic procedure for the preparation of OH-Pors **9**–**12**. Reagents and conditions: i) 3,4,5-trisdodecyloxybenzoic acid, *N*,*N*′-diisopropylcarbodiimide (DIPC), 4-(dimethylamino)pyridinium toluene-*p*-sulfonate (DPTS), tetrahydrofuran (THF)/CH_2Cl_2 1:2, 25 °C

Results and Discussion

Synthesis and Characterization of the OH-Por Precursors

The synthesis of the OH-Pors is outlined in Scheme 3. The molecules were prepared by treating 5,10,15,20-tetra(*p*-hydroxyphenyl)porphyrin with 2.2 equivalents of 3,4,5-trisdedocyloxybenzoic acid. Mixtures of the reference molecule (**8**) and compounds **9**, **10**, **11**, and **12** were obtained through this procedure; these were readily separated by flash column chromatography on silica gel as a result of the large polarity differences in **8**–**12**, thus resulting from the different number and positions of the −OH groups (polarity: **8** < **9** < **10** < **11** < **12**). The yields of these reactions were 13 (**8**), 13 (**9**), 13 (**10**), 19 (**11**), and 20% (**12**), with a total yield of all products of about 78% after purification. The molecular structures of **8**,[29] **9**, **10**, **11**, and **12** were characterized by ^{1}H and ^{13}C NMR spectroscopy and MALDI-TOF mass spectrometry. MALDI-TOF mass spectra clearly confirmed the structures of **9**, diOH-Por, and triOH-Por. The parent-ion peaks observed at *m*/*z* 2648.02, 1991.39, 1991.41, and 1334.43 in Figure S1 in the Supporting Information correspond to the molecular ions [M^+] of **9**, **10**, **11**, and **12**, respectively, and agree well with the calculated molecular weights of the corresponding molecules. Although the 5,15- and 5,10-isomers of the diOH-substituted compound cannot be distinguished from their MALDI-TOF mass spectra, their molecular symmetry is distinctly different and NMR spectroscopy experiments can readily distinguish between the two isomers. As shown in Figure 1, the molecular structure of **10** includes two twofold rotational axes, whereas **11** only has one. The difference in molecular symmetry leads to different chemical environments for the β protons on the pyrrole rings and different chemical shifts and splitting patterns in the ^{1}H NMR spectra. As a result, only one signal was observed at $\delta = 8.91$ ppm for the β protons of **10**, but three signals were observed at $\delta = 8.96$, 8.90, and 8.82 ppm for the β protons of **11** (Figure 1). Thus, from a combination of molecular characterization techniques, the molecular identities of **9**–**12** were established unambiguously.

Synthesis of the C_{60}–Por Shape Amphiphiles

As outlined in Scheme 4, the shape amphiphiles, mono-C_{60}Por (**1**), *trans*-diC_{60}Por (**2**), *cis*-diC_{60}Por (**3**), triC_{60}Por (**4**), and tetraC_{60}Por (**5**) were prepared by treating **9**, **10**, **11**, **12**, and **6** separately with **13** through a second Steglich esterification.

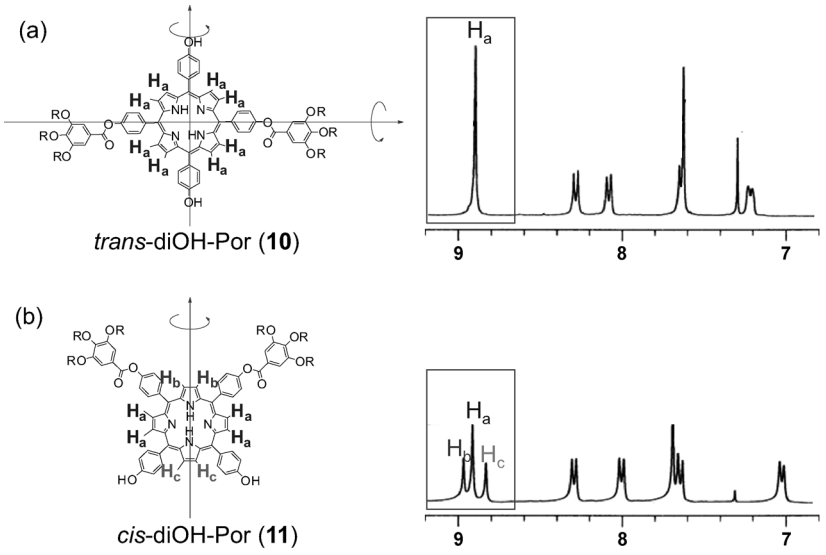

Figure 1. Molecular structures and ^{1}H NMR spectra of a) **10** and b) **11**.

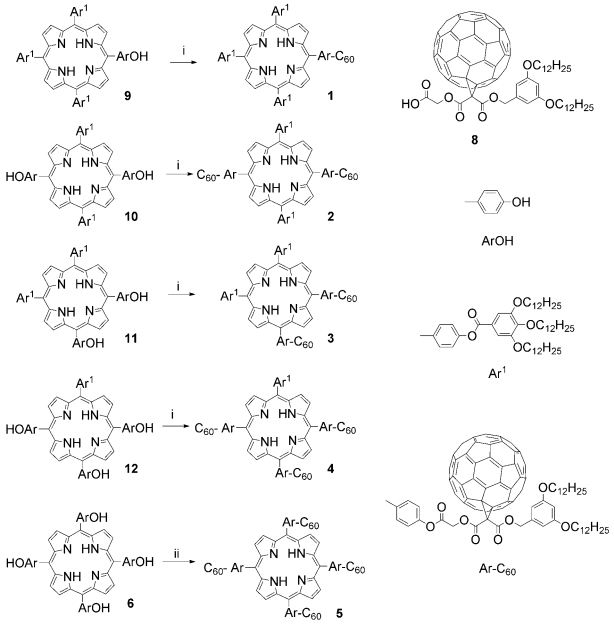

Scheme 4. Synthetic procedure for the preparation of C_{60}–Por shape amphiphiles **1**–**5**. Reagents and conditions: i) **13**, DIPC, DPTS, CH_2Cl_2, 25 °C; ii) **13**, DIPC, DPTS, THF/CH_2Cl_2 1:2, 25 °C.

The yields of each shape amphiphile after purification were 71 (**1**), 63 (**2**), 83 (**3**), 73 (**4**), and 53% (**5**). Comparisons of the ^{1}H NMR spectra of **9** and **1** are given in Figure 2a and b. After the esterification reaction, the protons on the *p*-hydroxyphenyl group of **9** ($\delta = 8.09$ and 7.21 ppm) shifted downfield to $\delta = 8.26$ and 7.60 ppm owing to the resonance effect of the electron-withdrawing carbonyl group, and the signals of the protons on the attached C_{60} arm appeared at $\delta = 6.68$, 6.46, 5.55, 5.37, and 3.94 ppm. In Figure S2 in the Supporting Information, the signals between $\delta = 136$ and 146 ppm in the ^{13}C NMR spectrum of **1** (Figure S2a) were not observed in the spectrum of **9** (Figure S2b); this clearly indicates the presence of the sp^2 carbons of the C_{60} unit. These results evidently imply the formation of an ester bond between the OH-Por precursor and **13**. The ^{1}H NMR spectra of **2**, **3**, **4**, and **5** are also shown in Figure 2c–f. The signal of the methylene groups next to the oxygen atom ($-OCH_2-$) on the 3,4,5-tris(dodecyloxy)benzoate of the Ar^1 arm appear at $\delta =$ 4.15–4.19 ppm. Comparing the integration of this signal to those protons belonging to the C_{60} units, it is clear that, as the number of C_{60} units per molecule increases, the integration of this signal decreases, whereas those signals belonging to the C_{60} arms show increased integration. In addition, differ-

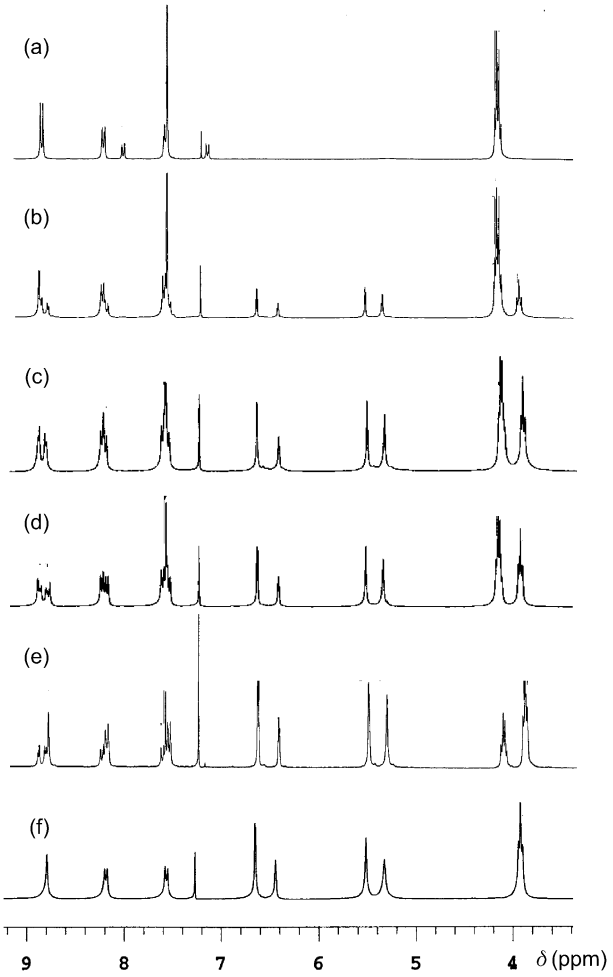

Figure 2. ^{1}H NMR spectra of a) **9**, b) **1**, c) **2**, d) **3**, e) **4**, and f) **5**.

ent molecular symmetries of **2** and **3** affect the signals of the β protons on the pyrrole rings of the Por core. In the region between $\delta = 8.8$ and 9.0 ppm, the β protons of the more symmetrical compound, **2**, has two doublet signals, whereas less symmetrical **3** has two groups of multiple signals. The MALDI-TOF mass spectra (Figures S3–S6 in the Supporting Information) have m/z values that closely match the molecular ions $[M^+]$ of each C_{60}–Por shape amphiphile. These combined results confirmed the success in obtaining the C_{60}–Por shape amphiphiles.

Photophysical Properties of the C_{60}–Por Shape Amphiphiles

The ground-state absorption spectra of the C_{60}–Por amphiphiles (**1**–**5**) and reference molecules **8** and **13** were examined in THF (Figure 3). Comparison of reference compounds **8** and **13** with **1**–**5** indicate little, if any, ground-state electronic coupling occurs between the two chromophores. The absorption spectra of **1**–**5** are similar to one another and are characterized by absorptions in the Q-band region at 515, 550, 590 and 646 nm, and in the more intense Soret band region at 419 nm. The two higher energy bands at $\lambda_{max} = 258$ and 326 nm result from the C_{60} groups and the intensity of these bands scales linearly with the number of C_{60} groups in each dyad.

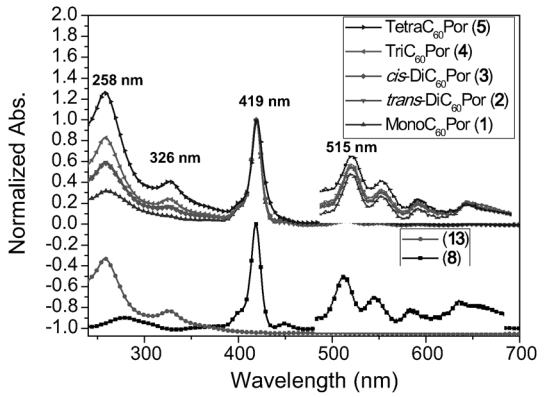

Figure 3. Normalized absorption spectra of the C_{60}–Por shape amphiphiles (**1**–**5**) and compounds **8** and **13** in THF.

Electronic coupling between the Por and C_{60} moieties in covalently bound C_{60}–Por derivatives typically leads to a bathochromic shift of the Soret and Q bands of the Por moiety.[42,60] The degree of the bathochromic shift depends on the relative spatial orientation of the C_{60} and Por moieties. Guldi et al. showed that C_{60}–Por dyads aligned in face-to-face orientations underwent bathochromic shifts to a greater extent than edge-to-face aligned C_{60}–Por dyads, most likely because of stronger Por-to-C_{60} electronic coupling present in the face-to-face aligned dyad.[42] In the case of **1**–**5**, bathochromic shifts were not observed in either the Soret or Q-band absorptions, relative to **8**. Thus, electronic coupling between Por and C_{60} in **1**–**5** is weak and the relative position of Por and C_{60} in **1**–**5** is likely to be close to an edge-to-face alignment. Considering the fact that the C_{60} moieties in **1**–**5** are connected to the Por core at only one point (instead of two points in the study by Guldi et al.),[42] the C_{60} groups in **1**–**5** are likely to be oriented away from the Por core; this accounts for the small Por-to-C_{60} electronic coupling and lack of a bathochromic shift in the absorption bands.

The generation of charge carriers is a critical step in the photon-to-electron conversion process in photovoltaic cells.[61] Previous studies have demonstrated the potential of C_{60}–Por dyads in photovoltaic applications,[36,37,45,46] in which the generation of long-lived charge carriers makes these materials an attractive component in bulk-heterojunction photovoltaics. Great interest lies in how the variation in the C_{60}/Por ratio affects the photophysical behavior of C_{60}–Por shape amphiphiles. Because quenching of the Por fluorescence (FL) in Por-containing donor–acceptor dyads is a good qualitative indicator of electron transfer, and therefore, of the generation of charge carriers,[39–41,43,62] we decided to examine the FL spectra of **1**–**5** (Figure 4). The FL spectrum of **8** is typical of tetraarylporphyrins, and has emission bands at $\lambda_{max} = 653$ and 721 nm (Figure 4a). The FL spectra of **1**–**5** displayed emission bands at the same energies, but with intensities significantly reduced relative to **8**. The FL quantum yields (Φ_{FL}) of each compound were deter-

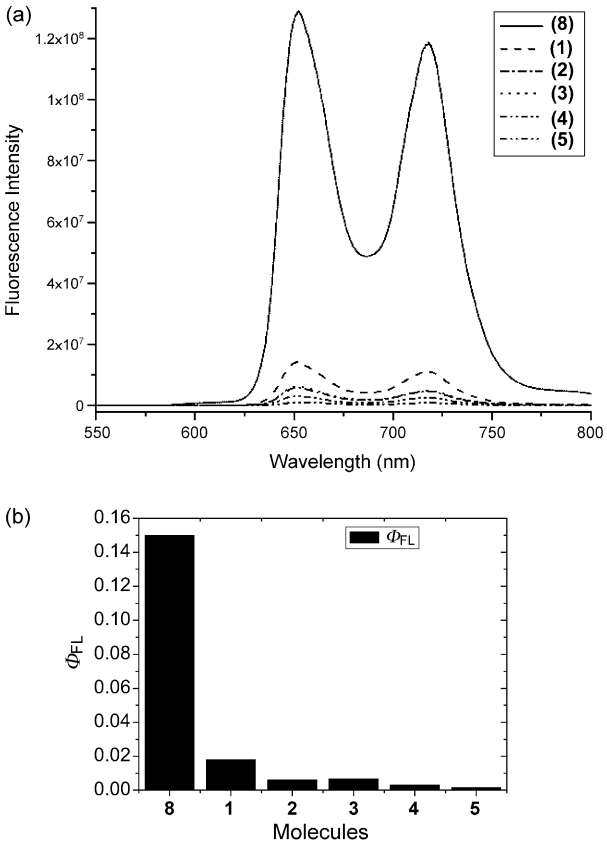

Figure 4. a) The FL spectra of **8** and dyads **1**–**5** in THF. b) The quantum yields (Φ_{FL}) are plotted as a function of the number of C_{60} groups.

mined and are shown graphically in Figure 4b. Interestingly, the Φ_{FL} values decrease from 0.15 for **8** to 0.018 for **1** and to about 0.001 for **5** as the number of C_{60} units increases from one in **1** to four in **5** (Figure 4b). The difference in Φ_{FL} between **2** and **3** is less pronounced. The significant decrease in Φ_{FL} in **1**–**5** as a function of the number of C_{60} groups present on the shape amphiphiles is consistent with previous work,[39–41,43,57] thus indicating efficient electron or energy transfer from photoexcited Por to the C_{60} group; this potentially leads to charge-separation ($Por^{+\cdot}C60^{-\cdot}$). The specific regiochemistry of the attachment points in multi-C_{60} bearing Por shape amphiphiles appears to play a less significant role. These preliminary results suggest the potential use of these C_{60}–Pors amphiphiles as photoinduced charge-generation materials in the active layer of photovoltaics. We are currently using transient absorption spectroscopy to determine charge-separation and recombination rate constants in these dyads.

Time-correlated single-photon counting (TCSPC) experiments were used to measure the Por excited-state lifetimes (τ) of **1**–**5** and reference compound **8**, and are summarized in Table 1. Excitation was performed at the Por Q-band absorption at 560 nm in THF in these experiments, whereas the Por emission band was monitored at 651 nm. As expected, the decay of **8** was monoexponential with a lifetime of 10.1 ns; this was consistent with the literature value of 10–11 ns for similar Pors.[63] The decays for dyads **1**–**5** were considerably shorter than that of **8** and were best fit by using two- or three-component global analysis (Table 1). The lifetime recorded for **1** is characterized by one longer-lived component of 2.16 ns comprising 86% of the decay and a second, shorter lifetime of 499 ps (9%). The data for **2** and **3**, which have two C_{60} groups positioned at either the 5,10- or 5,15-meso positions, show much shorter lifetime components of 1.16 ns (86%) and 331 ps (14%) for **2** and 1.29 ns (81%), and 427 ps (19%) for **3**. Similar effects were observed for **4** and **5**. From this information and the average lifetime (τ_{avg}) data reported in Table 1, it is clear that the addition of each C_{60} group leads to a decrease in the FL lifetime. These results are consistent with the Φ_{FL} data, which also showed a marked decrease in the Φ_{FL} values with each additional C_{60} group. On the basis of prior photophysical experiments on Por–C_{60} dyads in THF,[43,64–65] the decrease in the τ values of **1**–**5**, compared with **8**, were attributed to photoinduced electron transfer. Electron-transfer rate constants, k_{ET}, were calculated from the TCSPC data by using Equation (1):

$$k_{ET} = (1/\tau_{DA}) - (1/\tau_{D}) \quad (1)$$

in which τ_{DA} is the lifetime of **1**–**5** and τ_{D} represents the lifetime of model porphyrin **8**. The k_{ET} values shown in Table 1 were calculated by using τ_1 (k_{ET1}) and τ_2 (k_{ET2}), whereas $k_{ET(avg)}$ was calculated by using the average FL lifetime. In the case of **5**, the two shorter-lived lifetime components were used to calculate k_{ET1} and k_{ET2}. From this data, it is clear that the addition of each C_{60} group results in increases in k_{ET1} and k_{ET2}.

Table 1. Summary of time-resolved FL data for **8** and the shape amphiphiles **1**–**5** in THF.[a]

Compounds	Fluorescence lifetime				k_{ET1}	k_{ET2}	$k_{ET(avg)}$
	τ_1 [ns]	τ_2 [ns]	τ_3 [ns]	τ_{avg} [ns][b]	[s^{-1}]	[s^{-1}]	[s^{-1}]
8	10.1 (100%)			10.1			
1	2.16 (71%)	0.499 (29%)		2.02	0.36×10^9	1.91×10^9	0.40×10^9
2	1.16 (63%)	0.331 (37%)		1.04	0.76×10^9	2.92×10^9	0.86×10^9
3	1.29 (59%)	0.427 (41%)		1.13	0.68×10^9	2.24×10^9	0.79×10^9
4	0.769 (61%)	0.273 (39%)		0.68	1.20×10^9	3.56×10^9	1.38×10^9
5	1.25 (4.8%)	0.511 (43%)	0.109 (51%)	0.58	1.86×10^9	9.08×10^9	1.63×10^9

[a] An excitation wavelength of $\lambda_{ex}=560$ nm and an emission wavelength of $\lambda_{em}=651$ nm were used. [b] The average lifetimes were calculated by using the formula $\tau_{avg}=a_1\tau_1+a_2\tau_2+a_3\tau_3$, in which a_n represents the percentage of each decay component.

Conclusion

An effective two-step sequential esterification strategy was developed for the preparation of a series of C_{60}–Pors shape amphiphiles. The hydroxy-functionalized Por precursors (**9**–**12**) were prepared with high purity in a one-pot procedure and all of the C_{60}–Por shape amphiphiles (**1**–**5**) were readily synthesized in good yields in the subsequent Steglich esterification reaction with **13**. Photophysical studies showed that the UV/Vis absorption spectra of the C_{60}–Por shape amphiphiles obeyed the simple addition of the absorption of the C_{60} nanoparticles and the Por core. These results implied weak electronic coupling between the C_{60} and Por moieties and suggested that the relative orientation of the two moieties was close to the edge-to-face alignment. Compared with reference molecule **8**, the FL of the Por core in the C_{60}–Por shape amphiphiles was significantly quenched owing to the presence of the covalently bonded C_{60} units. The FL quenching became even more pronounced as the number of C_{60} units per molecule increased from one to four. TCSPC experiments also showed a decrease in τ and an increase in k_{ET} of the Por core with the addition of each C_{60} group. Photophysical studies suggested the potential for the effective generation of charge-separated species, $C_{60}^{-\cdot}Por^{+\cdot}$, from the photoexcited C_{60}–Por shape amphiphiles. Further investigations are ongoing with regard to phase behavior, phase structures, and the potential use of the C_{60}–Por shape amphiphiles as light harvesters and charge-carrier generators in optoelectronic applications.

Experimental Section

Instrumentation

All ^{1}H and ^{13}C NMR spectra were obtained with a Varian Gemini 300 spectrometer at 300 and 75 MHz, respectively. The ^{1}H NMR spectra were referenced to the residual proton impurities in the $CDCl_3$ at $\delta =$ 7.27 ppm. The ^{13}C NMR spectra were referenced to $^{13}CDCl_3$ at $\delta =$ 77.00 ppm. MALDI-TOF measurements were carried out on a Bruker Ultraflex III TOF instrument (Bruker Daltonics, Inc., Billarica, MA) equipped with a Nd:YAG laser emitting at a wavelength of 355 nm. All spectra were measured in the positive reflector mode. The instrument was calibrated prior to each measurement with external standards, poly(-methyl methacrylate) and polystyrene. Data analysis was carried out by using flexAnalysis software. Absorption spectra were obtained with a Shimadzu 1601 UV spectrometer. Steady-state FL measurements were performed on an ISA Jobin Yvon-SPEX Fluorolog 3-22 fluorometer with dual input and output monochromators. The samples were prepared in approximately micromolar concentrations in THF (Fischer Scientific, HPLC grade). FL spectra were collected as argon-saturated solutions by exciting at the Soret maxima in S/R mode to correct for changes in the lamp output intensity. FL spectra were also corrected for grating and detector response and were performed with 2.5 nm excitation and emission slit widths. Quantum yield measurements were made relative to tetraphenylporphyrin ($\Phi_{FL} = 0.11$). Time-resolved FL experiments were performed by using the TCSPC technique. The instrument used in this work utilized pulses from a Coherent cavity dumped 702 dye laser pumped by the 527 nm output of a continuous wave (CW) mode-locked Nd:YLF laser. The FL signal was detected at 54.7° with an emission polarizer and depolarizer by using a Hamamatsu R3809U-51 red-sensitive multichannel plate detector (MCP). Data collection and analysis were accomplished with an Edinburgh Instruments data collection system and the PicoQuant FluoFit decay analysis program, respectively. Time resolution on this instrument was estimated to be about 10 ps after reconvolution. Time-resolved decays were fit such that values of $\chi^2 < 1.20$ were obtained. Error limits in these measurements were estimated to be $\pm 10\%$. All TCSPC experiments were run in argon-saturated solutions in THF with optical densities of between 0.10 and 0.15 at the excitation wavelength (Q-band, λ_{ex} 560 nm) and with detection at $\lambda_{ex} = 651$ nm.

Materials

Unless otherwise noted, chemicals and solvents were purchased as reagent grade and used without further purification. CH_2Cl_2 was purchased from Acros as anhydrous grade. Toluene was dried over CaH_2 under argon and THF was dried over a mixture of sodium/benzophenone under argon. Both solvents were freshly distilled prior to use. 5,10,15,20-Tetra(*p*-hydroxyphenyl)porphyrin; 3,4,5-trisdodecyloxybenzoic acid; and the carboxylic acid derivative of methanofullerene (**13**) were prepared according to procedures reported in the literature.[29,56] The synthesis of **1**[46] and an analogue of **2**, *trans*-DiC_{60}Zn^{II}Por,[44] were reported in our previous work. The samples were kept in vacuum before characterization.

OH-Por Derivatives

3,4,5-Trisdodecyloxybenzoic acid (1.43 g, 2.12 mmol) was dissolved in CH_2Cl_2 (80 mL) and then slowly added to a solution of 5,10,15,20-tetra(*p*-hydroxyphenyl)porphyrin (0.80 g, 1.2 mmol), DIPC (318 mg, 2.50 mmol) and DPTS (633 mg, 2.12 mmol) in THF (40 mL) at 0 °C. After addition, the solution was stirred at room temperature for 1 day. The solvent was then removed in vacuo. The residue was dissolved in a mixture of CH_2Cl_2/hexanes (1:1) and subjected to column chromatography (SiO_2, hexanes/ethyl acetate (EA) 40:1 (v/v)). The products were eluted out with a mixture of EA and hexanes with different ratios as shown below. After chromatography, products were reprecipitated from a THF solution with MeOH.

*Compound **9***

Eluted with hexanes/EA = 8:1 (v/v); yield: 422 mg, 13%; ^{1}H NMR (300 MHz, $CDCl_3$): $\delta = 8.96$ (s, 4H), 8.93 (s, 4H), 8.30 (d, $J = 8.4$ Hz, 6H), 8.09 (d, $J = 8.4$ Hz, 2H), 7.65 (d, $J = 8.4$ Hz, 6H), 7.62 (s, 6H), 7.21 (d, $J = 8.4$ Hz, 2H), 4.20–4.13 (m, 18H), 1.97–1.82 (m, 18H), 1.58 (brs, 18H), 1.31 (brs, 144H), 0.92–0.88 (m, 27H), −2.75 ppm (s, 2H); ^{13}C NMR (75 MHz, $CDCl_3$): $\delta = 165.5$, 155.8, 153.8, 153.3, 151.2, 143.4, 139.9, 136.0, 135.6, 134.7, 124.2, 120.5, 120.3, 119.4, 119.2, 114.0, 109.0, 73.9, 69.6, 32.2, 32.1, 30.6, 30.0, 30.0, 29.9, 29.8, 29.7, 29.6, 29.6, 26.4, 26.3, 22.9, 14.4 ppm; HRMS (MALDI-TOF): *m*/*z* calcd for $C_{173}H_{258}N_4O_{16}$ $[M]^+$: 2647.95; found: 2647.98.

*Compound **10***

Eluted with hexanes/EA = 3:1 (v/v); yield: 308 mg, 13%; ^{1}H NMR (300 MHz, $CDCl_3$): $\delta = 8.91$ (s, 8H), 8.28 (d, $J = 8.4$ Hz, 4H), 8.07 (d, $J = 8.4$ Hz, 4H), 7.62 (d, $J = 8.4$ Hz, 4H), 7.61 (s, 4H), 7.19 (d, $J = 8.4$ Hz, 4H), 4.18–4.12 (m, 12H), 1.94–1.80 (m, 12H), 1.59 (brs, 12H), 1.30 (brs, 96H), 0.90–0.87 ppm (m, 18H); ^{13}C NMR (75 MHz, $CDCl_3$): $\delta = 165.7$, 155.8, 153.3, 151.1, 143.3, 140.0, 135.9, 135.6, 134.4, 124.1, 120.5, 120.3, 119.0, 113.9, 108.9, 73.9, 69.6, 32.2, 32.1, 30.6, 30.0, 29.9, 29.9, 29.8, 29.7, 29.6, 29.6, 26.4, 26.3, 22.9, 14.4 ppm; HRMS (MALDI-TOF): *m*/*z* calcd for $C_{130}H_{182}N_4O_{12}$ $[M]^+$: 1991.38; found: 1991.39.

*Compound **11***

Eluted with hexanes/EA = 3:1 (v/v); yield: 455 mg, 19%; ^{1}H NMR (300 MHz, $CDCl_3$): $\delta = 8.96$ (s, 2H), 8.90 (s, 4H), 8.82 (s, 2H), 8.28 (d, $J = 8.1$ Hz, 4H), 7.98 (d, $J = 8.1$ Hz, 4H), 7.66 (s, 4H), 7.61 (d, $J = 8.1$ Hz, 4H), 6.98 (d, $J = 8.1$ Hz, 4H), 4.22–4.18 (m, 12H), 1.99–1.84 (m, 12H), 1.59 (brs, 12H), 1.33 (brs, 96H), 0.94–0.89 ppm (m, 18H); ^{13}C NMR (75 MHz, $CDCl_3$): $\delta = 165.7$, 155.8, 153.3, 151.1, 143.3, 140.0, 135.9, 135.6, 134.4, 124.1, 120.5, 120.3, 119.0, 113.9, 108.9, 74.0, 69.6, 32.2, 32.1, 30.6, 30.0, 29.9, 29.9, 29.8, 29.7, 29.6, 29.6, 26.4, 26.3, 22.9, 14.4 ppm; HRMS (MALDI-TOF): *m*/*z* calcd for $C_{130}H_{182}N_4O_{12}$ $[M]^+$: 1991.38; found: 1991.41; $[M+23]^+$: *m*/*z* 2014.42.

*Compound **12***

Eluted with hexanes/EA = 2:1 (v/v); yield: 315 mg, 20%; ^{1}H NMR (300 MHz, $CDCl_3$): $\delta = 8.90$ (s, 4H), 8.86 (s, 4H), 8.28 (d, $J = 8.4$ Hz, 2H), 8.06–8.02 (m, 6H), 7.63–7.60 (m, 4H), 7.18–7.11 (m, 6H), 4.18–4.11 (m, 6H), 1.94–1.84 (m, 6H), 1.56 (brs, 6H), 1.43–1.30 (m, 48H), 0.93–0.88 ppm (m, 9H); ^{13}C NMR (75 MHz, $CDCl_3$): $\delta = 165.6$, 155.4, 153.1, 150.9, 143.3, 139.9, 135.6, 135.4, 134.5, 123.9, 120.1, 120.0, 119.9, 118.7, 113.6, 108.9, 73.8, 69.5, 32.0, 31.9, 30.4, 29.8, 29.8, 29.7, 29.7, 29.7, 29.6, 29.5, 29.4, 29.4, 29.4, 26.2, 26.1, 22.7, 22.7, 14.1, 14.1 ppm; HRMS (MALDI-TOF): *m*/*z* calcd for $C_{87}H_{106}N_4O_8$ $[M]^+$: 1334.80; found: 1334.43.

C_{60}–Por Shape Amphiphiles
*Compound **1***

Compound **13** (50 mg, 3.8×10^{-2} mmol), **9** (100 mg, 3.8×10^{-2} mmol), and DPTS (11 mg, 3.8×10^{-2} mmol) were dissolved in CH_2Cl_2 (10 mL) and cooled to 0 °C. DIPC (5.6 mg, 4.5×10^{-2} mmol) was slowly added into the solution by using a microsyringe. The solution was stirred at room temperature for 1 day. The solvent was then removed in vacuo. The residue was dissolved in hexanes/EA = 20:1 and subjected to column chromatography (SiO_2, hexanes/EA = 20:1 (v/v)) to allow isolation of **1**. The obtained dark brown fraction was then concentrated. The product was dissolved in CH_2Cl_2 and precipitated in acetone as a dark brown solid (106 mg, 71%). ^{1}H NMR (300 MHz, $CDCl_3$): $\delta = 8.96$ (s, 4H), 8.94 (d, $J = 5.1$ Hz, 2H), 8.87 (d, $J = 5.1$ Hz, 2H), 8.30 (d, $J = 8.4$ Hz, 6H), 8.26 (d, $J = 8.7$ Hz, 2H), 7.65 (d, $J = 8.4$ Hz, 6H), 7.62 (s, 6H), 7.60 (d, $J = 8.4$ Hz, 2H), 6.68 (d, $J = 1.8$ Hz, 2H), 6.46 (brs, 1H), 5.55 (s, 2H), 5.37 (s, 2H), 4.19–4.15 (m, 18H), 3.94 (t, $J = 6.6$ Hz, 4H), 1.96–1.71 (m, 22H), 1.58 (brs, 18H), 1.30–1.21 (m, 180H), 0.91–0.83 (m, 33H), −2.78 ppm (s, 2H); ^{13}C NMR (75 MHz, $CDCl_3$): $\delta = 165.4$, 163.4, 163.2, 160.7, 153.3, 151.3, 150.1, 145.3, 145.1, 144.8, 144.8, 144.7, 143.9, 143.4, 143.1, 143.0, 142.2, 142.0, 141.9, 141.1, 141.0, 140.5, 139.8, 138.9, 136.8, 135.7, 124.2, 120.4, 119.8, 119.6, 119.1, 108.9, 107.5, 101.9, 73.9, 71.3, 69.6, 68.4, 63.1, 32.2, 32.1, 30.6, 30.0, 30.0, 29.9, 29.8, 29.7, 29.6, 29.6, 29.5, 26.4, 26.3, 22.9, 22.9, 14.4 ppm; HRMS (MALDI-TOF): *m*/*z* calcd for $C_{269}H_{314}N_4O_{23}$ $[M]^+$: 3968.35; found: 3968.29.

Compound ***2***

Compound **13** (86 mg, 6.4×10^{-2} mmol), **10** (58 mg, 2.9×10^{-2} mmol), and DPTS (18 mg, 6.1×10^{-2} mmol) were dissolved in CH_2Cl_2 (10 mL) and cooled to 0 °C. DIPC (9.6 mg, 7.7×10^{-2} mmol) was slowly added into the solution by using a microsyringe. The solution was stirred at room temperature for 1 day. The solvent was then removed in vacuo. The residue was dissolved in CH_2Cl_2 and subjected to column chromatography (SiO_2, CH_2Cl_2/THF = 20:1 (v/v)) to allow isolation of **2**. The obtained dark brown fraction was then concentrated. The product was dissolved in CH_2Cl_2 and precipitated in acetone as a black solid (91 mg, 63 %). ^{1}H NMR (300 MHz, $CDCl_3$): δ = 8.93 (d, J = 4.5 Hz, 4H), 8.85 (d, J = 4.5 Hz, 4H), 8.29–8.23 (m, 8H), 7.66–7.58 (m, 12H), 6.68 (d, J = 1.8 Hz, 4H), 6.45 (brs, 2H), 5.54 (s, 4H), 5.36 (s, 4H), 4.18–4.12 (12H, m), 3.93 (t, J = 6.3 Hz, 8H), 1.93–1.71 (m, 20H), 1.58 (brs, 12H), 1.30–1.21 (m, 168H), 0.91–0.83 (m, 30H), −2.82 ppm (s, 2H); ^{13}C NMR (75 MHz, $CDCl_3$): δ = 165.5, 165.4, 163.4, 163.2, 160.7, 153.3, 151.3, 150.1, 145.3, 145.1, 145.1, 145.0, 144.8, 144.7, 144.6, 143.9, 143.3, 143.1, 143.0, 143.0, 142.2, 142.0, 141.9, 141.0, 140.9, 140.5, 139.7, 138.9, 136.8, 135.7, 124.2, 120.4, 119.9, 119.7, 119.2, 108.9, 107.5, 101.9, 73.9, 71.3, 69.5, 68.4, 63.1, 32.2, 32.1, 30.6, 30.0, 30.0, 29.9, 29.8, 29.8, 29.7, 29.6, 29.6, 29.5, 26.4, 26.3, 22.9, 22.9, 14.4 ppm; HRMS (MALDI-TOF): m/z calcd for $C_{322}H_{294}N_4O_{26}$ $[M]^+$: 4632.18; found: 4632.19.

Compound ***3***

Compound **13** (105 mg, 7.8×10^{-2} mmole), **11** (75 mg, 3.8×10^{-2} mmol), and DPTS (18 mg, 6.1×10^{-2} mmol) were dissolved in CH_2Cl_2 (10 mL) and cooled to 0 °C. DIPC (12 mg, 9.4×10^{-2} mmol) was slowly added into the solution by using a microsyringe. The solution was stirred at room temperature for 1 day. The solvent was then removed in vacuo. The residue was dissolved in CH_2Cl_2 and subjected to column chromatography (SiO_2, CH_2Cl_2/THF 20:1 (v/v)) to allow isolation of **3**. The obtained dark brown fraction was then concentrated. The product was dissolved in CH_2Cl_2 and precipitated in acetone as a black solid (150 mg, 83 %). ^{1}H NMR (300 MHz, $CDCl_3$): δ = 8.93 (m, 4H), 8.84 (m, 4H), 8.28 (d, J = 8.4 Hz, 4H), 8.26 (d, J = 8.4 Hz, 4H), 7.66–7.57 (m, 12H), 6.67 (d, J = 1.5 Hz, 4H), 6.45 (brs, 2H), 5.53 (s, 4H), 5.36 (s, 4H), 4.18–4.12 (12H, m), 3.93 (t, J = 6.6 Hz, 8H), 1.93–1.71 (m, 20H), 1.58 (brs, 12H), 1.30–1.21 (m, 168H), 0.91–0.83 (m, 30H), −2.82 ppm (s, 2H); ^{13}C NMR (75 MHz, $CDCl_3$): δ = 165.5, 165.4, 163.4, 163.2, 160.8, 153.3, 151.3, 150.1, 145.2, 145.2, 145.1, 145.1, 144.8, 144.7, 144.6, 144.6, 144.6, 143.8, 143.8, 143.4, 143.0, 143.0, 143.0, 142.9, 142.1, 142.0, 141.9, 141.0, 140.9, 140.5, 139.8, 139.7, 138.9, 136.8, 135.7, 124.2, 120.4, 119.9, 119.8, 119.2, 108.9, 107.5, 101.9, 73.9, 71.3, 69.6, 69.5, 68.4, 63.1, 32.2, 32.1, 30.6, 30.0, 29.9, 29.9, 29.7, 29.6, 29.6, 29.5, 26.4, 23.0, 14.4 ppm; HRMS (MALDI-TOF): m/z calcd for $C_{322}H_{294}N_4O_{26}$ $[M]^+$: 4632.18; found: 4632.22.

Compound ***4***

Compound **13** (118 mg, 8.8×10^{-2} mmole), **12** (38 mg, 2.8×10^{-2} mmol), and DPTS (25 mg, 8.5×10^{-2} mmol) were dissolved in CH_2Cl_2 (10 mL) and cooled to 0 °C. DIPC (13 mg, 1.0×10^{-1} mmol) was slowly added into the solution by using a microsyringe. The solution was stirred at room temperature for 1 day. The solvent was then removed in vacuo. The residue was dissolved in CH_2Cl_2 and subjected to column chromatography (SiO_2, CH_2Cl_2/THF = 10:1 (v/v)) to allow isolation of **4**. The obtained dark brown fraction was then concentrated. The product was dissolved in CH_2Cl_2 and precipitated in acetone as a black solid (114 mg, 73 %). ^{1}H NMR (300 MHz, $CDCl_3$): δ = 8.91 (d, J = 4.8, 2H), 8.84 (d, J = 4.8, 2H), 8.81 (s, 4H), 8.26 (d, J = 8.4, 2H), 8.23–8.19 (m, 6H), 7.64 (d, J = 8.4 Hz, 2H), 7.61(s, 2H), 7.58 (d, J = 8.4 Hz, 6H), 6.66 (d, J = 2.1 Hz, 6H), 6.45 (t, J = 2.1 Hz, 3H), 5.53 (s, 6H), 5.34 (s, 6H), 4.18–4.12 (6H, m), 3.93 (t, J = 6.6 Hz, 12H), 1.92–1.75 (m, 18H), 1.55 (brs, 6H), 1.42–1.22 (m, 156H), 0.91–0.83 (m, 27H), −2.82 ppm (s, 2H); ^{13}C NMR (75 MHz, $CDCl_3$): δ = 165.5, 163.4, 163.2, 160.8, 153.3, 151.3, 150.1, 145.2, 145.2, 145.1, 145.0, 144.8, 144.7, 144.6, 144.5, 143.8, 143.8, 143.7, 143.0, 143.0, 142.9, 142.9, 142.1, 142.0, 141.9, 141.0, 141.0, 140.5, 139.7, 138.9, 136.8, 135.7, 124.2, 120.4, 119.9, 119.3, 109.0, 107.5, 101.9, 73.9, 71.3, 69.6, 69.4, 68.4, 63.1, 32.2, 32.1, 30.6, 30.0, 30.0, 29.9, 29.8, 29.7, 29.6, 29.6, 29.5, 26.4, 22.9, 22.9, 14.4 ppm; HRMS (MALDI-TOF): m/z calcd for $C_{375}H_{275}N_4O_{29}$ $[M+H]^+$: 5297.02; found: 5297.04.

Compound ***5***

Compound **13** (120 mg, 9.0×10^{-2} mmol), 5,10,15,20-tetra(*p*-hydroxyphenyl)porphyrin (14 mg, 2.1×10^{-2} mmol), and DPTS (24 mg, 8.4×10^{-2} mmol) were dissolved in THF/CH_2Cl_2 (1:2, 12 mL v/v) and cooled to 0 °C. DIPC (14 mg, 1.1×10^{-1} mmol) was slowly added into the solution by using a microsyringe. The solution was stirred at room temperature for 2 days. The solvent was then removed in vacuo. The residue was dissolved in CH_2Cl_2 and subjected to column chromatography (SiO_2, CH_2Cl_2/THF = 10:1 (v/v)) to allow isolation of **5**. The obtained dark brown fraction was then concentrated. The product was dissolved in CH_2Cl_2 and precipitated in acetone as a black solid (71 mg, 53 %). ^{1}H NMR (300 MHz, $CDCl_3$): δ = 8.79 (s, 8H), 8.18 (d, J = 8.1, 8H), 7.56 (d, J = 8.1 Hz, 8H), 6.65 (d, J = 1.5 Hz, 8H), 6.44 (brs, 4H), 5.52 (s, 8H), 5.33 (s, 8H), 3.92 (t, J = 6.3 Hz, 16H), 1.78–1.73 (m, 16H), 1.43 (brs, 16H), 1.23 (brs, 128H), 0.858 (t, J = 6.6 Hz, 24H), −2.82 ppm (s, 2H); ^{13}C NMR (75 MHz, $CDCl_3$): δ = 165.5, 163.4, 163.2, 160.7, 150.1, 145.1, 145.0, 144.9, 144.6, 144.5, 144.4, 144.3, 143.7, 143.6, 142.9, 142.9, 142.8, 142.8, 142.7, 142.0, 141.8, 141.7, 140.9, 140.8, 140.4, 139.6, 138.9, 136.8, 135.7, 119.9, 119.4, 107.5, 101.8, 71.2, 69.4, 68.4, 63.1, 51.3, 32.1, 29.9, 29.9, 29.7, 29.6, 29.5, 26.4, 22.9, 14.4 ppm; HRMS (MALDI-TOF): m/z calcd for $C_{428}H_{255}N_4O_{32}$ $[M+H]^+$: 5960.84; found: 5960.93.

Acknowledgements

This work was supported by the National Science Foundation (DMR-0906898, S.Z.D.C. and CHE-0216371, D.A.M.), the Collaborative Center for Polymer Photonics, AFOSR, the Joint-Hope Foundation, and the National Science Council of Taiwan (NSC100-2221-E-009-152-MY3). We appreciate Dr. Xiaopeng Li and Prof. Chrys Wesdemiotis for assistance with the MALDI-TOF mass spectra measurements.

[1] J.-M. Lehn, *Proc. Natl. Acad. Sci. USA* **2002**, *99*, 4763–4768.
[2] G. Whitesides, J. Mathias, C. Seto, *Science* **1991**, *254*, 1312–1319.
[3] L. Brunsveld, J. A. J. M. Vekemans, J. H. K. K. Hirschberg, R. P. Sijbesma, E. W. Meijer, *Proc. Natl. Acad. Sci. USA* **2002**, *99*, 4977–4982.
[4] S. Leininger, B. Olenyuk, P. J. Stang, *Chem. Rev.* **2000**, *100*, 853–908.
[5] M. Antonietti, S. Förster, *Adv. Mater.* **2003**, *15*, 1323–1333.
[6] D. Philp, J. F. Stoddart, *Angew. Chem.* **1996**, *108*, 1242–1286; *Angew. Chem. Int. Ed. Engl.* **1996**, *35*, 1154–1196.
[7] G. Ungar, C. Tschierske, V. Abetz, R. Holyst, M. A. Bates, F. Liu, M. Prehm, R. Kieffer, X. Zeng, M. Walker, *Adv. Funct. Mater.* **2011**, *21*, 1296–1323.
[8] J. A. A. W. Elemans, R. van Hameren, R. J. M. Nolte, A. E. Rowan, *Adv. Mater.* **2006**, *18*, 1251–1266.
[9] M. R. Wasielewski, *Acc. Chem. Res.* **2009**, *42*, 1910–1921.
[10] P. Samorì, F. Cacialli, H. L. Anderson, A. E. Rowan, *Adv. Mater.* **2006**, *18*, 1235–1238.
[11] X. Zhang, S. Rehm, M. M. Safont-Sempere, F. Würthner, *Nat. Chem.* **2009**, *1*, 623–629.
[12] Y. Yamamoto, G. Zhang, W. Jin, T. Fukushima, N. Ishii, A. Saeki, S. Seki, S. Tagawa, T. Minari, K. Tsukagoshi, T. Aida, *Proc. Natl. Acad. Sci. USA* **2009**, *106*, 21051–21056.
[13] P. Samorì, A. Fechtenkötter, E. Reuther, M. D. Watson, N. Severin, K. Müllen, J. P. Rabe, *Adv. Mater.* **2006**, *18*, 1317–1321.
[14] R. Bhosale, J. Misek, N. Sakai, S. Matile, *Chem. Soc. Rev.* **2010**, *39*, 138–149.
[15] W. Richard, D. W. Bruce, *J. Am. Chem. Soc.* **2003**, *125*, 9012–9013.
[16] M. A. Horsch, Z. Zhang, S. C. Glotzer, *Phys. Rev. Lett.* **2005**, *95*, 056105.
[17] Z. Zhang, M. A. Horsch, M. H. Lamm, S. C. Glotzer, *Nano Lett.* **2003**, *3*, 1341–1346.
[18] P. H. J. Kouwer, G. H. Mehl, *J. Mater. Chem.* **2009**, *19*, 1564–1575.

[19] C. Tschierske, D. J. Photinos, *J. Mater. Chem.* **2010**, *20*, 4263–4294.
[20] X. Yu, S. Zhong, X. Li, Y. Tu, S. Yang, R. M. Van Horn, C. Ni, D. J. Pochan, R. P. Quirk, C. Wesdemiotis, W.-B. Zhang, S. Z. D. Cheng, *J. Am. Chem. Soc.* **2010**, *132*, 16741–16744.
[21] Y. Li, W.-B. Zhang, I. F. Hsieh, G. Zhang, Y. Cao, X. Li, C. Wesdemiotis, B. Lotz, H. Xiong, S. Z. D. Cheng, *J. Am. Chem. Soc.* **2011**, *133*, 10712–10715.
[22] H. J. Sun, Y. Tu, C. L. Wang, R. M. Van Horn, C. C. Tsai, M. J. Graham, B. Sun, B. Lotz, W. B. Zhang, S. Z. D. Cheng, *J. Mater. Chem.* **2011**, *21*, 14240–14247.
[23] W.-B. Zhang, Y. Li, X. Li, X. Dong, X. Yu, C.-L. Wang, C. Wesdemiotis, R. P. Quirk, S. Z. D. Cheng, *Macromolecules* **2011**, *44*, 2589–2596.
[24] X. Yu, W.-B. Zhang, K. Yue, X. Li, H. Liu, Y. Xin, C. L. Wang, C. Wesdemiotis, S. Z. D. Cheng, *J. Am. Chem. Soc.* **2012**, *134*, 7780–7787.
[25] X. Dong, W.-B. Zhang, Y. Li, M. Huang, S. Zhang, R. P. Quirk, S. Z. D. Cheng, *Polym. Chem.* **2012**, *3*, 124–134.
[26] J. He, K. Yue, Y. Liu, P. Ni, K. A. Cavicchi, R. P. Quirk, E.-Q. Chen, S. Z. D. Cheng, W.-B. Zhang, *Polym. Chem.* **2012**, *3*, 2112–2120.
[27] Y. Li, X. Dong, K. Guo, Z. Wang, Z. Chen, C. Wesdemiotis, R. P. Quirk, W.-B. Zhang, S. Z. D. Cheng, *ACS Macro Lett.* **2012**, *1*, 834–839.
[28] S. Laschat, A. Baro, N. Steinke, F. Giesselmann, C. Hägele, G. Scalia, R. Judele, E. Kapatsina, S. Sauer, A. Schreivogel, M. Tosoni, *Angew. Chem.* **2007**, *119*, 4916–4973; *Angew. Chem. Int. Ed.* **2007**, *46*, 4832–4887.
[29] X. Zhou, S.-W. Kang, S. Kumar, R. R. Kulkarni, S. Z. D. Cheng, Q. Li, *Chem. Mater.* **2008**, *20*, 3551–3553.
[30] P. A. Heiney, J. E. Fischer, A. R. McGhie, W. J. Romanow, A. M. Denenstein, J. P. McCauley, Jr., A. B. Smith, D. E. Cox, *Phys. Rev. Lett.* **1991**, *66*, 2911–2914.
[31] T. G. Linssen, K. Durr, M. Hanack, A. J. Hirsch, *Chem. Soc. Chem. Commun.* **1995**, 103–104.
[32] T. Fukuda, S. Masuda, N. Kobayashi, *J. Am. Chem. Soc.* **2007**, *129*, 5472–5479.
[33] D. I. Schuster, K. Li, D. M. Guldi, A. Palkar, L. Echegoyen, C. Stanisky, R. J. Cross, M. Niemi, N. V. Tkachenko, H. Lemmetyinen, *J. Am. Chem. Soc.* **2007**, *129*, 15973–15982.
[34] F. Wessendorf, B. Grimm, D. M. Guldi, A. Hirsch, *J. Am. Chem. Soc.* **2010**, *132*, 10786–10795.
[35] G. de Miguel, M. Wielopolski, D. I. Schuster, M. A. Fazio, O. P. Lee, C. K. Haley, A. L. Ortiz, L. Echegoyen, T. Clark, D. M. Guldi, *J. Am. Chem. Soc.* **2011**, *133*, 13036–13054.
[36] H. Hayashi, W. Nihashi, T. Umeyama, Y. Matano, S. Seki, Y. Shimizu, H. Imahori, *J. Am. Chem. Soc.* **2011**, *133*, 10736–10739.
[37] R. Charvet, Y. Yamamoto, T. Sasaki, J. Kim, K. Kato, M. Takata, A. Saeki, S. Seki, T. Aida, *J. Am. Chem. Soc.* **2012**, *134*, 2524–2527.
[38] G. Liu, A. N. Khlobystov, G. Charalambidis, A. G. Coutsolelos, G. A. D. Briggs, K. Porfyrakis, *J. Am. Chem. Soc.* **2012**, *134*, 1938–1941.
[39] H. Imahori, K. Hagiwara, M. Aoki, T. Akiyama, S. Taniguchi, T. Okada, M. Shirakawa, Y. Sakata, *J. Am. Chem. Soc.* **1996**, *118*, 11771–11782.
[40] H. Imahori, Y. Sakata, *Adv. Mater.* **1997**, *9*, 537–546.
[41] C. Luo, D. M. Guldi, H. Imahori, K. Tamaki, Y. Sakata, *J. Am. Chem. Soc.* **2000**, *122*, 6535–6551.
[42] D. M. Guldi, C. Luo, M. Prato, A. Troisi, F. Zerbetto, M. Scheloske, E. Dietel, W. Bauer, A. Hirsch, *J. Am. Chem. Soc.* **2001**, *123*, 9166–9167.
[43] S. Schlundt, G. Kuzmanich, F. Spänig, G. de Miguel Rojas, C. Kovacs, M. A. Garcia-Garibay, D. M. Guldi, A. Hirsch, *Chem. Eur. J.* **2009**, *15*, 12223–12233.
[44] C.-L. Wang, W.-B. Zhang, C.-H. Hsu, H.-J. Sun, R. M. Van Horn, Y. Tu, D. V. Anokhin, D. A. Ivanov, S. Z. D. Cheng, *Soft Matter* **2011**, *7*, 6135–6143.
[45] C.-L. Wang, W.-B. Zhang, R. M. Van Horn, Y. Tu, X. Gong, S. Z. D. Cheng, Y. Sun, M. Tong, J. Seo, B. B. Y. Hsu, A. J. Heeger, *Adv. Mater.* **2011**, *23*, 2951–2956.
[46] C.-L. Wang, W.-B. Zhang, H.-J. Sun, R. M. Van Horn, R. R. Kulkarni, C.-C. Tsai, C.-S. Hsu, B. Lotz, X. Gong, S. Z. D. Cheng, *Adv. Energy Mater.* **2012**, *2*, 1375–1382.
[47] J.-F. Nierengarten, C. Schall, J.-F. Nicoud, *Angew. Chem.* **1998**, *110*, 2037–2040; *Angew. Chem. Int. Ed.* **1998**, *37*, 1934–1936.
[48] M. Urbani, J.-F. Nierengarten, *Tetrahedron Lett.* **2007**, *48*, 8111–8115.
[49] M. Urbani, J. Iehl, I. Osinska, R. Louis, M. Holler, J.-F. Nierengarten, *Eur. J. Org. Chem.* **2009**, 3715–3725.
[50] J.-F. Nierengarten, L. Oswald, J.-F. Nicoud, *Chem. Commun.* **1998**, 1545–1546.
[51] A. D. Adler, F. R. Longo, J. D. Finarelli, J. Goldmacher, J. Assour, L. Korsakoff, *J. Org. Chem.* **1967**, *32*, 476–476.
[52] J. S. Lindsey, I. C. Schreiman, H. C. Hsu, P. C. Kearney, A. M. Marguerettaz, *J. Org. Chem.* **1987**, *52*, 827–836.
[53] J. Iehl, R. Pereira de Freitas, B. Delavaux-Nicot, J.-F. Nierengarten, *Chem. Commun.* **2008**, 2450–2452.
[54] M. A. Fazio, O. P. Lee, D. I. Schuster, *Org. Lett.* **2008**, *10*, 4979–4982.
[55] J. D. Megiatto, R. Spencer, Jr., D. I. Schuster, *Org. Lett.* **2009**, *11*, 4152–4155.
[56] J. Iehl, I. Osinska, R. Louis, M. Holler, J.-F. Nierengarten, *Tetrahedron Lett.* **2009**, *50*, 2245–2248.
[57] J. Iehl, M. Vartanian, M. Holler, J.-F. Nierengarten, B. Delavaux-Nicot, J.-M. Strub, A. Van Dorsselaer, Y. Wu, J. Mohanraj, K. Yoosaf, N. Armaroli, *J. Mater. Chem.* **2011**, *21*, 1562–1573.
[58] D. Felder, H. Nierengarten, J.-P. Gisselbrecht, C. Boudon, E. Leize, J.-F. Nicoud, M. Gross, A. Van Dorsselaer, J.-F. Nierengarten, *New J. Chem.* **2000**, *24*, 687–695.
[59] J. Petersson, M. Eklund, J. Davidsson, L. Hammarström, *J. Am. Chem. Soc.* **2009**, *131*, 7940–7941.
[60] E. Dietel, A. Hirsch, E. Eichhorn, A. Rieker, S. Hackbarth, B. Roder, *Chem. Commun.* **1998**, 1981–1982.
[61] Y.-J. Cheng, S.-H. Yang, C.-S. Hsu, *Chem. Rev.* **2009**, *109*, 5868–5923.
[62] D. M. Guldi, C. Luo, M. Prato, E. Dietel, A. Hirsch, *Chem. Commun.* **2000**, 373–374.
[63] J. Rodriguez, C. Kirmaier, D. Holten, *J. Am. Chem. Soc.* **1989**, *111*, 6500–6506.
[64] F. D'Souza, S. Gadde, A. L. Schumacher, M. E. Zandler, A. S. D. Sandanayaka, Y. Araki, O. Ito, *J. Phys. Chem. C* **2007**, *111*, 11123–11130.
[65] H. Imahori, K. Tamaki, D. M. Guldi, C. Luo, M. Fujitsuka, O. Ito, Y. Sakata, S. Fukuzumi, *J. Am. Chem. Soc.* **2001**, *123*, 2607–2617.

Received: November 15, 2012
Published online: February 20, 2013